

J/ψ and $\psi(2S)$ production in small systems with PHENIX

Anthony D Frawley, on behalf of the PHENIX collaboration

Department of Physics, Florida State University, Tallahassee Florida 32306, USA.

Received 15 January 2022; accepted 4 May 2022

The nuclear modification of J/ψ production has been studied at forward and backward rapidity in the collision systems p +Al, p +Au, and ^3He +Au. A comparison of results for p +Au and ^3He +Au is presented, with a focus on possible differences caused by the different particle multiplicity in the final state. The modification of $\psi(2S)$ production in p +Au collisions has also been studied at forward and backward rapidity as a function of centrality. The $\psi(2S)$ results complement earlier results at mid-rapidity at RHIC energies and results obtained at LHC energies, revealing a strong rapidity dependence of the $\psi(2S)$ nuclear modification at RHIC energies that is indicative of final state effects.

Keywords: RHIC energie; J/ψ and $\psi(2S)$ production; PHENIX.

1. Introduction

Recent quarkonium analyses in PHENIX have focused on data from small collision systems, obtained during the RHIC 2014 and 2015 runs. The goal of these analyses has been to shed light on two questions: do we see evidence of final state effects in light systems, and how well do we understand charmonium nuclear modification in light systems?

There was a long-standing expectation in the field that measurements of the nuclear modification in p +A collisions could establish an independent baseline for the modification of charmonium production in A + A collisions. This assumed that production in p +A collisions was dominated by what were referred to as “cold nuclear matter” (CNM) effects, for example modifications of the gluon distributions in nuclei [1,2], nuclear “absorption” (breakup of the forming charmonium [6]. But this idea was cast into doubt by two observations. Strong modification of the $\psi(2S)$ relative to the J/ψ was observed by PHENIX in midrapidity data at RHIC energy [7], something that did not seem to be consistent with CNM effects alone. Similar results were later found in p +Pb collisions at LHC energies [8,9]. The second was the observation of flow-like behavior in p +Pb collisions at the LHC and, later, in p +Au, d +Au, and ^3He +Au collisions at RHIC [10-14].

At RHIC energies, PHENIX has reported J/ψ and $\psi(2S)$ modifications at the rapidities $1.2 < |y| < 2.2$ in p +Au, ^3He +Au and p +Al collisions [15-17]. PHENIX has also reported J/ψ modifications in d +Au collisions at those rapidities [18,19], as well as $\psi(2S)$ modifications in d +Au collisions at $|y| < 0.35$ [7]. Star has reported d +Au J/ψ modifications at $|y| < 1$ [20].

In p +Pb collisions at LHC energies, the nuclear modification for the J/ψ and $\psi(2S)$ has been reported by ALICE [8,21-24] and LHCb [9,25]. There are also J/ψ and $\psi(2S)$ modifications from ATLAS [26,27] and CMS [28,29], however those measurements do not extend to low transverse momentum where final state effects should be most important.

The PHENIX results described here extended the available data sample to include measurements at RHIC energy of a) $\psi(2S)$ modification in p +Au collisions at forward and backward rapidity for the first time, and b) comparison of the nuclear modification of J/ψ production in p +Au and ^3He +Au collisions to look for evidence of final state effects.

2. Experiment

The $J/\psi \rightarrow \mu^+\mu^-$ and $\psi(2S) \rightarrow \mu^+\mu^-$ data discussed here were measured in the PHENIX muon arms at $\sqrt{s_{NN}} = 200$ GeV for the collisions $p + p$, p +Al, p +Au, and ^3He +Au, during the RHIC runs in 2014 and 2015. The integrated luminosity was 47 pb^{-1} for $p + p$, 590 nb^{-1} for p +Al, 138 nb^{-1} for p +Au, and 18 nb^{-1} for ^3He +Au collisions. The measurement and analysis details for the J/ψ results are described in [30], those for the $\psi(2S)$ in [17].

3. J/ψ results

First, we consider the question of whether the additional energy production in ^3He +Au collisions produces a measurable effect on the nuclear modification. Figure 1 presents a comparison of the nuclear modification versus transverse momentum for inclusive J/ψ in p +Au and ^3He +Au in the 0 – 20% most central collisions. The lower panels show the ratio of modifications for the two systems. At forward rapidity the ratio is consistent with unity within 5%. At backward rapidity, where final state effects would be expected to be most important, the ratio is consistent with some additional suppression in ^3He +Au (probability 90%), but is not far outside the systematic uncertainty. The results indicate that final state suppression due to the larger final state multiplicity of ^3He +Au is small, at most.

Next, we consider how well the modification of J/ψ production can be described by CNM effects alone. Figure 2 shows transverse momentum and centrality integrated data for p +Al, p +Au, and ^3He +Au collisions. The data are compared with calculations by Shao *et. al* of the modification

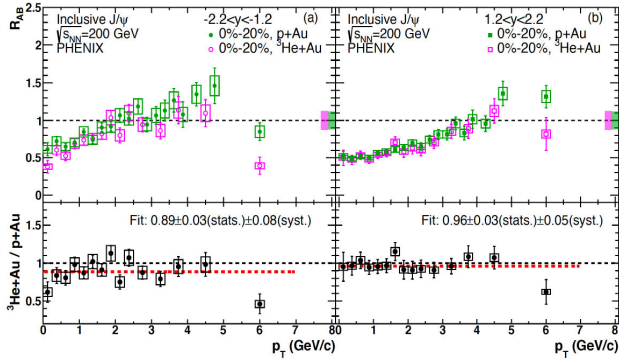


FIGURE 1. Comparison of the nuclear modification of J/ψ production in p +Au and ^3He +Au collisions for the 20% most central collisions.

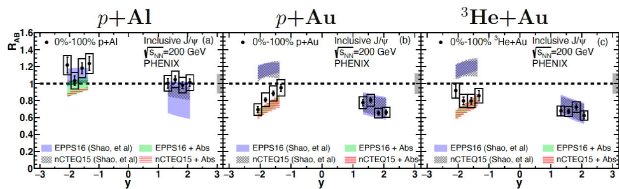


FIGURE 2. The centrality and transverse momentum integrated modification of J/ψ production in p +Al, p +Au and ^3He +Au collisions. The calculations are discussed in the text.

due to the EPPS16 [1] and nCETQ15 [2] gluon shadowing parameterizations, modified using a Bayesian reweighting method to add constraints from LHC p +Pb J/ψ data [31-35]. The reweighting procedure uses data that is expected to be dominated by gluon shadowing alone. The theoretical uncertainties reflect the 68% confidence level, and are based on the scale uncertainty. These calculations describe the forward rapidity data for all systems, and the backward rapidity data for the p +Al collisions. The data for the Au target cases are not reproduced at backward rapidity by the shadowing calculation. It is expected that at backward rapidity, due to the much lower relative rapidity of the target nucleons and the forming charmonium, the expanding charmonium will approach its final size while still in the target, and may be broken up by collisions with nucleons. An estimate of this so called “absorption” cross section, derived from fits to shadowing corrected data across a broad range of energies in [3], has been folded with the shadowing calculations and included in Fig. 2. The combination of shadowing and nuclear absorption at backward rapidity reproduces the data reasonably well.

In summary, comparison of the p +Au and ^3He +Au modifications shows little difference, and they are well described by CNM effects - namely predictions from gluon shadowing at forward rapidity, and gluon shadowing folded with nuclear absorption at backward rapidity.

4. $\psi(2S)$ results

Because of the much lower binding energy of the $\psi(2S)$, it is expected to be more susceptible to final state effects than the

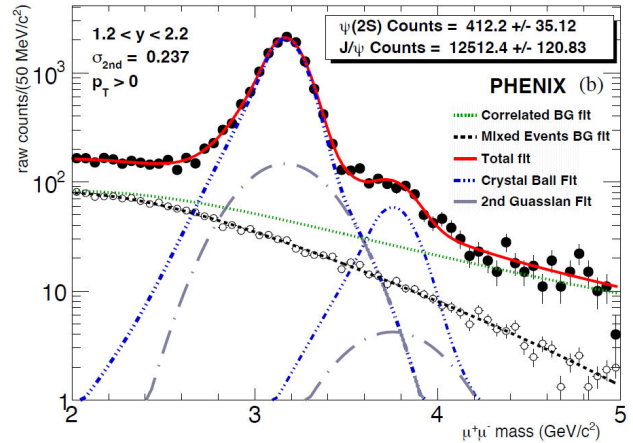


FIGURE 3. Example of the invariant mass spectrum from p +Au collisions at forward rapidity. The fitted curves are Crystal Ball lineshape fits to the J/ψ and $\psi(2S)$ peaks, along with various estimated background sources.

J/ψ . Indeed this seems to be born out in the available data from RHIC and LHC experiments. A recent analysis of PHENIX data from the 2015 RHIC p +Au run provided adequate statistical precision to extract a meaningful $\psi(2S)$ modification versus centrality at forward and backward rapidity [17], for the first time at RHIC. This complements the earlier d +Au data from PHENIX at midrapidity [7].

The invariant mass spectrum at forward rapidity is shown in Fig. 3. The details of the fit procedure and uncertainty analysis can be found in [17].

The rapidity dependence of the J/ψ and $\psi(2S)$ modification in p +Au collisions, integrated over centrality is shown in Fig. 4. The modifications at forward rapidity are very similar for the two states, while at backward rapidity the $\psi(2S)$ is much more strongly suppressed. Predictions of the modification due to gluon shadowing by Shao *et al* for both states are shown for comparison. The shadowing calculations are very similar for the two states, predicting slightly more suppression of the $\psi(2S)$ at forward rapidity, and slightly less

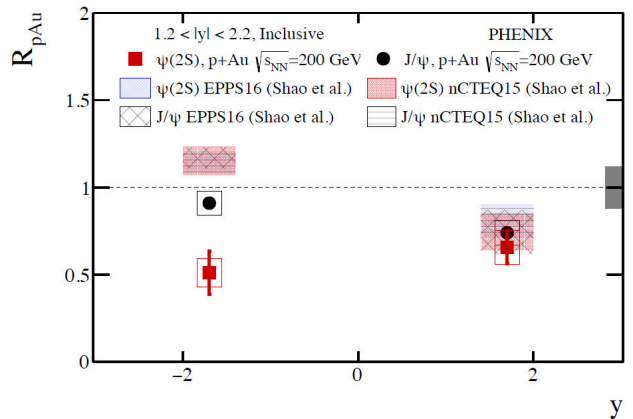


FIGURE 4. Nuclear modification of the J/ψ and $\psi(2S)$ in p +Au collisions as a function of rapidity, integrated over centrality. The theory calculations are discussed in the text.

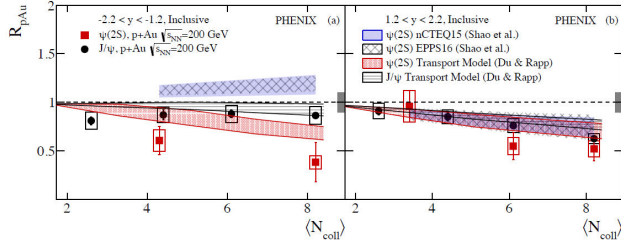


FIGURE 5. Nuclear modification of the J/ψ and $\psi(2S)$ in $p+Au$ collisions as a function of centrality. The model calculations are discussed in the text.

suppression of the $\psi(2S)$ at backward rapidity. The calculations are in good agreement with the data at forward rapidity, but sit well above the measured modifications at backward rapidity. As shown earlier, addition of a nuclear absorption estimate to the shadowing for the J/ψ reproduces the data reasonably well. We do not have a nuclear absorption estimate for the $\psi(2S)$, but the absorption model used for the J/ψ necessarily produces very similar suppression estimates for the $\psi(2S)$. CNM effects do not seem to be able to explain the stronger suppression of the $\psi(2S)$.

The centrality dependence of the measured nuclear modification of the $\psi(2S)$ is compared with that of the J/ψ in Fig. 5. The $\psi(2S)$ suppression is only slightly greater than that of the J/ψ at forward rapidity, but it is markedly lower at backward rapidity. Also included in Fig. 5 are shadowing predictions by Shao *et al.* for the J/ψ and $\psi(2S)$. The shadowing predictions are in reasonable agreement with the data at forward rapidity, but at backward rapidity the predicted modification is much larger than the measured one. In the case of the J/ψ this is likely due to the absence of nuclear absorption in the calculations.

Also shown in Fig. 5 are transport model calculations by Du and Rapp [36]. The transport model has been extended to small systems, having been developed for A+A collisions to describe the evolution of charmonium as it passes through expanding hot nuclear matter [37]. The model includes estimates using the EPS09 parameterization of the CNM modification due to gluon shadowing, as well as a nuclear absorption estimate based on the PHENIX $d+Au$ J/ψ data. The estimated contributions from CNM effects - which are assumed to be the same for J/ψ and $\psi(2S)$ - are shown in each case as a solid line. Adding the reweighted EPPS16 and nCTEQ15 shadowing estimates in Fig. 6 shows that the shadowing estimate alone seems to account for the data reasonably well at forward rapidity, perhaps slightly underpredicting the $\psi(2S)$ suppression. At backward rapidity, where both antishadowing and nuclear absorption are important, the CNM effects included in the transport model describe the J/ψ data reasonably well. For the $\psi(2S)$ case, at backward rapidity the model predicts significant final state effects, although they are not as strong as in the data. The calculated ratio of the $\psi(2S)$ and J/ψ modifications is close to that in the data, so it may be that the CNM estimates in the Du and Rapp calculation are responsible for at least part of the difference.

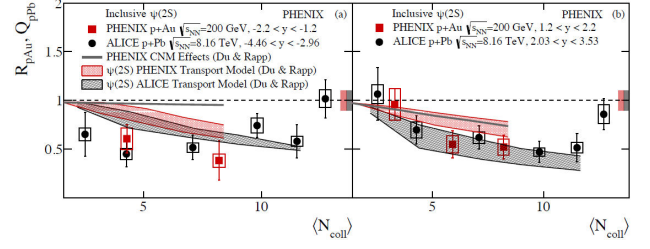


FIGURE 6. Comparison of the nuclear modification of the J/ψ and $\psi(2S)$ in $p+Au$ collisions from PHENIX and $p+Pb$ collisions from ALICE. The model calculations are discussed in the text.

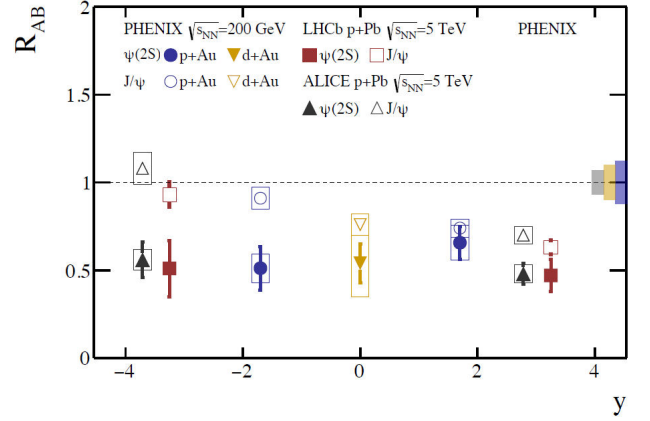


FIGURE 7. Comparison of the nuclear modification of the J/ψ and $\psi(2S)$ versus rapidity in $p+Au$ and $d+Au$ collisions from PHENIX and $p+Pb$ collisions from ALICE and LHCb.

It is interesting to compare the $\psi(2S)$ data from PHENIX with that from ALICE [24]. Figure 6 shows the centrality dependence comparison at forward and backward rapidity, with transport model comparisons from Du and Rapp [36]. The data from the two experiments are not directly comparable due to the much higher energy at the LHC. At the LHC, the nucleon-nucleon cross section is higher, leading to a larger range of $\langle N_{coll} \rangle$ values. Also the Bjorken x values probed in the ALICE data are smaller, and the Q^2 values are higher due to the larger average transverse momentum. Despite the differences in conditions, the measured modifications are similar between the two experiments. At backward rapidity, where final state effects dominate in the calculations, the suppressions predicted by the transport model are also similar.

Figure 7 compares the nuclear modification of the two states, integrated over rapidity and transverse momentum, for light collision systems as a function of rapidity. It includes data from PHENIX, ALICE [8,22] and LHCb [9,25]. The trend of increasing differential suppression of the $\psi(2S)$ as the rapidity decreases is striking, particularly so given that the data are at a mix of collision energies.

5. Summary

PHENIX J/ψ data from $p+Au$ collisions are reasonably well described by the Bayesian reweighted shadowing predictions

of Shao et al, with the addition of a nuclear absorption correction at backward rapidity. Comparison of J/ψ modifications from p +Au and ^3He +Au for the 0-20% most central collisions showed no difference at forward rapidity, within errors of 5%. At backward rapidity, the data are consistent with an additional suppression of about 10% in the ^3He +Au case, but the difference is barely outside the systematic uncertainty, and is not compelling.

The $\psi(2S)$ p +A data from PHENIX, ALICE and LHCb show only small additional suppression relative to the J/ψ at forward rapidity, and the data seem to be reasonably well described by CNM predictions. At backward rapidity - the heavy ion going direction - the $\psi(2S)$ is suppressed by roughly a factor of two relative to the J/ψ . The strong differential suppression at backward rapidity is not explained by CNM effects, but models including final state effects, such as the one by Du and Rapp shown here, can produce the effect.

-
1. K. J. Eskola, P. Paakkinen, H. Paukkunen, and C. A. Salgado. EPPS16: Nuclear parton distributions with LHC data. *Eur. Phys. J. C*, **77** (2017) 163.
 2. K. Kovarik *et al.*, nCTEQ15- Global analysis of nuclear parton distributions with uncertainties in the CTEQ framework. *Phys. Rev. D*, **93** (2016) 085037.
 3. D. C. McGlinchey, A. D. Frawley, and R. Vogt. Impact parameter dependence of the nuclear modification of J/ψ production in d+Au collisions at $\sqrt{pSNN} = 200$ GeV. *Phys. Rev. C*, **87** (2013) 054910.
 4. F. Arleo, P. B. Gossiaux, T. Gousset, and J. Aichelin. Charmo228 nium suppression in pA collisions. *Phys. Rev. C*, **61** (2000) 054906.
 5. I. Vitev. Non-Abelian energy loss in cold nuclear matter. *Phys. Rev. C* **75** (2007) 064906.
 6. J. W. Cronin *et al.*, Production of hadrons with large transverse momentum at 200, 300, and 400 GeV. *Phys. Rev. D*, **11** (1975) 3105.
 7. A. Adare *et al.* Nuclear Modification of ψ , χ_c and J/ψ Production in d+Au Collisions at $p\sqrt{sNN}=200$ GeV. *Phys. Rev. Lett.*, **111** (2013) 202301.
 8. B. Bezverkhny Abelev *et al.* Suppression of (2S) production in p-Pb collisions at $p\sqrt{sNN} = 5.02$ TeV. *JHEP*, **12** (2014) 073.
 9. R. Aaij *et al.*, Study of (2S) production and cold nuclear matter effects in pPb collisions at $p\sqrt{sNN} = 5$ TeV. *JHEP*, **03** (2016) 133.
 10. J. L. Nagle and W. A. Zajc, Small System Collectivity in Relativistic Hadronic and Nuclear Collisions. *Ann. Rev. Nucl. Part. Sci.*, **68** (2018) 211-235.
 11. V. Khachatryan *et al.* Observation of Long-Range Near- Side Angular Correlations in Proton-Proton Collisions at the LHC. *JHEP* **09** (2010) 091.
 12. B. Abelev *et al.* Long-range angular correlations on the near and away side in p-Pb collisions at $p\sqrt{sNN} = 5.02$ TeV. *Phys. Lett. B*, **719** (2013) 29-41.
 13. L. Adamczyk *et al.* Measurement of elliptic flow of light nuclei at $p\sqrt{sNN} = 200, 62.4, 39, 27, 19.6, 11.5, \text{ and } 7.7$ GeV at the BNL Relativistic Heavy Ion Collider. *Phys. Rev. C*, **94** (2016) 034908.
 14. M. Aaboud *et al.* Measurement of multi-particle azimuthal correlations in pp, p+Pb and low-multiplicity Pb+Pb collisions with the ATLAS detector. *Eur. Phys. J. C* **77** (2017) 428.
 15. U. Acharya *et al.* Measurement of J/ψ at forward and backward rapidity in p + p, p+Al, p+Au, and 3He+Au collisions at $p\sqrt{sNN} = 200$ GeV. *Phys. Rev. C* **102** (2020) 014902.
 16. A. Adare *et al.* Measurement of the relative yields of (2S) to 265 (1S) mesons produced at forward and backward rapidity in p + p, p+Al, p+Au, and 3He+Au collisions at $p\sqrt{sNN} = 200$ GeV. *Phys. Rev. C* **95** (2017) 034904.
 17. U. A. Acharya *et al.* Measurement of (2S) nuclear modification at backward and forward rapidity in p+p, p+Al, and p+Au collisions at $p\sqrt{sNN} = 200$ GeV. **2** (2022).
 18. A. Adare *et al.* Cold Nuclear Matter Effects on J/ψ Yields as a Function of Rapidity and Nuclear Geometry in Deuteron-Gold Collisions at $p\sqrt{sNN} = 200$ GeV. *Phys. Rev. Lett.*, **107** (2011) 142301.
 19. A. Adare *et al.* Transverse-Momentum Dependence of the J/ψ Nuclear Modification in d+Au Collisions at $p\sqrt{sNN} = 200$ GeV. *Phys. Rev. C*, **87** (2013) 034904.
 20. L. Adamczyk *et al.* J/ψ production at low transverse momentum in p+p and d+Au collisions at $p\sqrt{sNN} = 200$ GeV. *Phys. Rev. C*, **93** (2016) 064904.
 21. J. Adam *et al.* Centrality dependence of inclusive J/ψ production in p-Pb collisions at $p\sqrt{sNN} = 5.02$ TeV. *JHEP*, **11** (2015) 127.
 22. B. Bezverkhny Abelev *et al.* J/ψ production and nuclear effects in p-Pb collisions at $p\sqrt{sNN} = 5.02$ TeV. *JHEP*, **02** (2014) 073 .
 23. J. Adam *et al.* Centrality dependence of (2S) suppression in p-Pb collisions at $p\sqrt{sNN} = 5.02$ TeV. *JHEP*, **06** (2016) 050.
 24. S. Acharya *et al.* Centrality dependence of J/ψ and (2S) production and nuclear modification in p-Pb collisions at $p\sqrt{sNN} = 8.16$ TeV. *JHEP*, **02** (2021) 002.
 25. R. Aaij *et al.* Study of J/ψ production and cold nuclear matter effects in pPb collisions at $\sqrt{sNN} = 5$ TeV. *JHEP*, **02** (2014) 072.
 26. G. Aad *et al.* Measurement of differential J/ψ production cross sections and forward-backward ratios in p+Pb collisions with the ATLAS detector. *Phys. Rev. C*, **92** (2015) 034904.
 27. M. Aaboud *et al.* Measurement of quarkonium production in proton Slead and proton 300 proton collisions at 5:02 TeV with the ATLAS detector. *Eur. Phys. J. C*, **78** (2018) 171.
 28. A. M Sirunyan *et al.* Measurement of prompt and nonprompt J/ψ production in pp and pPb collisions at $\sqrt{sNN} = 5.02$ TeV. *Eur. Phys. J. C*, **77** (2017) 269.

29. A. M Sirunyan *et al.* Measurement of prompt (2S) production cross sections in proton-lead and proton-proton collisions at $\sqrt{s_{NN}} = 5.02$ TeV. *Phys. Lett. B*, **790** (2019) 509.
30. U. Acharya *et al.* Measurement of J/ψ at forward and backward rapidity in p+p, p+Al, p+Au, and 3He+Au collisions at $\sqrt{s_{NN}} = 200$ GeV. *Phys. Rev. C* **102** (2020) 014902.
31. A. Kusina, J.-P. Lansberg, I. Schienbein, and H.-S. Shao, Gluon Shadowing in Heavy-Flavor Production at the LHC. *Phys. Rev. Lett.* **121** (2018) 052004.
32. H.-S. Shao. HELAC-Onia: An automatic matrix element generator for heavy quarkonium physics. *Comput. Phys. Commun.* **184** (2013) 2562.
33. H.-S. Shao, HELAC-Onia 2.0: an upgraded matrix-element and event generator for heavy quarkonium physics. *Comput. Phys. Commun.* **198** (2016) 238.
34. J.-P. Lansberg and H.-S. Shao, Towards an automated tool to evaluate the impact of the nuclear modification of the gluon density on quarkonium, D and B meson production in proton-nucleus collisions. *Eur. Phys. J. C* **77** (2017) 1.
35. A. Kusina, Jean-Philippe Lansberg, Ingo Schienbein, and Hua-Sheng Shao. Reweighted nuclear PDFs using Heavy-Flavor Production Data at the LHC: nCTEQ15rwHF and EPPS16rwHF, (2020).
36. X. Du and R. Rapp, In-Medium Charmonium Production in Proton-Nucleus Collisions. *JHEP* **03** (2019) 015.
37. X. Zhao and R. Rapp, Charmonium in Medium: From Correlators to Experiment. *Phys. Rev. C*, **82** (2010) 064905.